Scanning electron microscopy analyses of an ITER plasma-facing unit mockup exposed to extreme ion fluences in Magnum-PSI

M. Balden[a,*], S. Elgeti[a], T.W. Morgan[b], S. Brezinsek[c], G. De Temmerman[d]

[a]*Max-Planck-Institut für Plasmaphysik, Boltzmanstr. 2, D-85748 Garching, Germany*
[b]*Dutch Institute for Fundamental Energy Research, Eindhoven, The Netherlands*
[c]*Forschungszentrum Jülich, Institut für Energie- und Klimaforschung-Plasmaphysik, D-52425 Jülich, Germany*
[d]*ITER Organization, Route de Vinon sur Verdon, CS 90 046, 13067 Saint Paul-Lez-Durance, Cedex France*

Abstract

A small-scale tungsten monoblock mockup was exposed to continuous Magnum-PSI plasma beams for 6 different condition: including pure H, D, and He plasmas as well as mixed D/He plasmas with low electron temperature (1.5-5 eV), with maximum surface temperatures up to 1250 °C, and ion fluences up to ~10^{30} m^{-2}. The recrystallization in the centre of the hottest exposure spots, the absence of cracking on all monoblocks, the formation of a several microns thick nanostructured fuzz layer by pure He exposure, and the presence of various impurities from the exposure in Magnum-PSI on the surface were observed and analysed with a dedicated scanning electron microscope able to handle the entire mockup without any cutting before.

1. Introduction

Finding a solution for the heat and particle removal from a fusion reactor is a key issue of present-day fusion research. Most of the research is traditionally focused on heat exhaust and influences of high heat loads on the material. Whereas these can be matched routinely in high heat flux test facilities, the ITER divertor components will be additionally exposed to unprecedented ion fluences [1]. Little data is currently available on the effect of high flux, high fluence on the morphology, hydrogen retention, and thermal and mechanical properties of tungsten (W). This is in particular true for the case of actively cooled components, for which the thermal gradient will affect the diffusion into the bulk. Following the installation of superconducting magnetic field coils at Magnum-PSI, it is now possible for the first time to explore the high fluence regime within reasonable machine time of ~20 h continuous exposure [2, 3].

The current plan for the start of ITER operation is the so-called “staged approach”, whereby the machine will progressively be brought up to full power operations. The plan is to have two non-active operational phases, in which hydrogen (H) and helium (He) plasmas will be used to commission the different systems and develop scenarios for the deuterium (D) – tritium (T) operation [4]. Resulting from that, some loading conditions representative for the different ITER operational phases were selected and led to an experimental proposal within the EUROfusion consortium [5] to mimic the ITER start-up phase. The exposures were performed in Magnum-PSI on a small-scale mockup of the ITER divertor plasma-facing units, consisting of seven tungsten monoblocks brazed on to a CuCrZr cooling tube. Six continuous exposures were performed on different W monoblocks with pure H, D, and He plasmas as well as mixed D/He plasmas at low electron temperature (1.5-5 eV) with maximum surface temperatures up to 1250 °C, and ion fluences up to ~10^{30} m^{-2}, which is of the order of the fluence expected over ~5000 full power Q_{DT}=10 discharges (400 s) [1]. More details about exposure conditions can be found in [6].

Detailed microscopy analyses can shed light on important questions regarding, e.g., recrystallization, He-induced nanostructured fuzz formation and deposited impurities. To avoid artefacts by sample preparation (especially by cutting) and to select areas of highest interest for further analyses, the entire mockup (as exposed) was analysed by a scanning electron microscope (SEM). The SEM used in the study is dedicated for analysing large and heavy samples (up to 10 kg, 23×10×6 cm^3) with the

capability to prepare cross-sections by focused ion beam (FIB) cutting and to perform elemental analyses with energy-dispersive X-ray spectroscopy (EDX).

This contribution describes the results of the SEM analyses assisted by confocal laser scanning microscopy (CLSM) on the entire mockup with emphasis on: (i) re-crystallization in the centre of the hottest exposed areas, (ii) absence of cracking on all monoblocks, (iii) formation of a nanostructured fuzz layer (several microns thick) due to pure He exposure, and (iv) presence of various impurities on the surface due to exposure in Magnum-PSI. These analyses will be followed by metallographic analyses on cross-sections achieved by cutting the component into pieces. First results from these cross-sections are discussed in [6].

2. Experimental

2.1 Sample

The exposed water-cooled small-scale mockup is prepared regarding the specification for ITER plasma facing units [7]. It is composed of a chain of 7 W monoblock (21×28×12 mm^2 block with 0.5 mm spacing) produced by Plansee and brazed onto a CuCrZr tube with a Cu interlayer. The sample is from the same series used in previous high heat flux studies [8].

2.2. Magnum exposure

The quasi continuous plasma exposures were performed in Magnum-PSI (with interruption during the night) [2, 3, 6]. Details for the six exposures are given in Tab. **1**. The surface temperatures T_{surf} indicated here are those measured using an infrared camera and a multi-wavelength pyrometer at the centre of the plasma beam (details see [9]). After the first three exposures onto the front side with their beam centre on every other monoblock, the mockup was flipped by 180° and the last three exposures were performed onto the backside. The exposures on every other monoblock should ensure that the exposures were done on nearly virgin surface while performing enough different conditions. Fig. **1** shows photos of both sides together with marks of the beam centre for the 6 exposures and the analyses positions performed in the frame of the presented study. The different surfaces of the monoblocks are named by F1-7 and B1-7 for the front side and the backside, respectively, and the exposures by the position of the beam centre. The beam width (FWHM) is of the order of 10-15 mm with a tail leading to features correlated to an exposure with a diameter of about 30 mm, see the halo on B3 and B5 of exposure B4 and on F4 and F6 of exposure F5 (Fig. **1**). More details to the exposures can be found in [6].

2.3. Characterisation by microscopy

The complex conditions of the wall loading in fusion devices by power and particles leads to various surface modifications of the plasma-facing components (PFCs). The clarification of the surface morphology and inner structures in near surface volumes requires detailed microscopy investigations. Non-destructive analyses are mandatory for sequential testing by analysing the same area before and after plasma exposure, i.e., the complete component as installed in the fusion device must fit into the microscope. Therefore, a scanning electron microscope (SEM / Auriga60 from ZEISS) with focused ion beam (FIB) and analytics, energy and wavelength dispersive X-ray spectroscopy (EDX/WDX from Bruker), was commissioned and put into operation at Max-Planck-Institut für Plasmaphysik. This SEM is equipped with a specially developed heavy-duty stage from Kammrath&Weiss, which allows to analyse samples up to a mass of 10 kg with an image resolution of < 5 nm. A sample of 23×10×6 cm^3 can be analysed without operational restrictions, i.e., the X-Y stage allows to access completely an area on the sample of 23×10 cm^2. The maximal sample size is 44 cm in length, 27 cm in width, and 10 cm without rotation module in height. Cross-sections can be prepared by FIB. A multiple gas injection system enables to deposit W, Pt, or C dominated markers, e.g., for erosion

measurements. Elemental mapping by EDX/WDX is possible also on cross-sections. Small features can be investigated by using a low energy electron beam (2-5 keV).

The SEM analyses on the entire mockup were performed with this dedicated "Auriga" SEM. The analyses positions of only imaging of the surface, elemental mapping, and imaging of FIB-prepared cross-sections are marked in Fig. **1** as "SEM", "EDX", and "CS", respectively.

In addition, a confocal laser scanning microscope (CLSM / LEXT OLS4000 from Olympus) was used to perform overviews of the surface by optical digital microscopy, to search for possible cracks (and melted surfaces) and to visualize the grain structure on the surface. Furthermore, the achievable height measurements with the laser unit were performed on selected areas. The position for detailed CLSM analyses are marked in Fig. **1**, too.

3. Results and discussion

3.1 Prelude: base material

As the surfaces of the mockup were not pre-characterized before the Magnum-PSI exposures, the centre of the surface F1 was taking as reference for an "unexposed" surface. This area is quite far away from the next centre of an exposure beam (>25 mm) receiving a very low heat load, avoiding any change in microstructure of the W material. Nevertheless, some impurity deposition onto the surface is observed, mainly molybdenum (Mo) (see section 3.5).

Fig. **2** shows this area and a cross-section in that region. Clearly, the grinding grooves of a technical surface finishing are visible with a roughness on the µm scale (R_q=0.6-1.2 µm; R_z=4-10 µm). Below the surface, a distorted layer with small grains (<<1 µm) on top are found (layer thickness ~3 µm). This layer extends over the full observation depth achieved in the performed cross-section of about 20 µm. The grain size at that depth exceeds easily 10 µm, leading to observation limitations on FIB-prepared cross-sections. More details will be obtained by the analyses on cross-sections after cutting the mockup. From first observations on such cross-sections, a grain size for the base material is of the order of 50-100 µm with some areas in between with grains of ~10 µm [6].

The observation of small grains close to the surface and a distorted layers up to the depth of the FIB-prepared cross-sections on F1 is confirmed on FIB-prepared cross-sections on B7, B3, F3 and B5 (Fig. **1**). The power load on at least the two former surfaces was low.

3.2 General surface inspection

In the inspection of surface with CLSM, the expected absence of cracking (and melting) was confirmed: no cracks (or melt traces) were observed, either in the beam centres or at the monoblock edges (obscured by grinding grooves, which are preserved). Special care with CLSM was exercised on three surfaces exposed at the highest temperatures (~1200 °C) (F5, B6, B2), where recrystallization could reduce the mechanical properties (see section 3.3). SEM analyses, which were not as extensive as with CLSM regarding the analysed area size but therefore with higher resolution, confirm the absence of cracking (and melting).

3.3 Recrystallization

Special emphasis was paid to the question whether recrystallization took place. The mechanical performance of W is degraded by recrystallization, especially its brittleness and, therefore, its cracking behaviour which could lead to severe damage of the plasma-facing components. Fig. **3** shows as an example the spot centre of the highest fluence exposure (~10^{30} m^{-2}) with T_{surf}>1200 °C. Note, at this temperature, complete recrystallization occurs for various W materials already after 1 h, and it is expected for the used one [8]. Clearly, recrystallized grains of 10-30 µm in size are detected on the surface (also in CLSM, not shown), even if the survived surface topography by the grinding hinders

the detection (Fig. **3**(a,b)). From CLSM data, the recrystallized grains on the surface extent over an area of roughly 1 cm^2.

In cross-sections (Figs. **3**(c-e)), the grain structure is strongly altered up to the full observation depth of 10-15 µm compared to the base material (Fig. **2**). The grains are distortion-free and extent beyond the analysable depth on the FIB-prepared cross-sections. These observations are independent whether the surface was exposed with pure D or with He addition in the plasma if the surface temperature was ~1200 °C. Larger depth will be accessible by analyses on metallographic cross-sections and an assessment of the recrystallization temperature under these loading conditions can be made [6].

3.4 Surface morphology changes by He

Clearly, the pure He exposure changes the surface morphology as is already observable by naked eye: the exposed area got black (B4, Figs. **1** and **4**(a)). In SEM, typical He-induced nanostructured fuzz is observed at T_{surf}~850 °C (Fig. **4**) despite the rather low ion energy (<18 eV due to floating conditions [6]), which is below the energy required for fuzz formation [10, 11]. Note that Mo is incorporated in the fuzz (see section 3.5.3; Fig. **4**(e)). Addition of He as for the exposures of blocks F7 and B6 with mixture D+He does not lead to fuzz formation, which potentially could be formed as found for high energy mixed H+He exposure [12]. Note the W surface structure of the mixed exposures (F7 and B6) is not distinguishable from that one of the pure D exposures at the same surface temperature of ~1200 °C (F5 and B2); see section 3.3.

The thickness of the fuzz layer across the blackish spot was analysed by a series of FIB-prepared cross-sections (Figs. **1** and **4**(a)). Interestingly, the layer is thinner in the centre of the spot (~3 µm) than at the edge (~8 µm) (Fig. **4**(c)), even if the structure of the fuzz on the surface and in the cross-section is the same. This could possibly understood by ion energy variations resulting from plasma potential variation across the plasma beam (dip in the centre).

In addition, the fuzz does not form anymore a continuous layer at the edge of the spot. These structures can be described as fuzz balls (Fig. **4**(f)). Possibly, they have a similar origin as the reported nano-tendril bundles [13, 14], which grow as isolated filigrane structures with high ratio height to lateral size on the W surface under various conditions.

As the neighbouring monoblock edge across a gap receive nearly the same impacting particle fluxes, but the total power deposited on each block is strongly different, and, therefore, the surface temperature differs strongly between these two edge regions (Figs. **4**(d, h)). This leads in the case from block B4 to B5 to a drop of the temperature by ~300 K so that the conditions for fuzz formation are not fulfilled anymore (below 800 K), i.e., no blackish area on block B5 (Fig. **4**(a)). Nevertheless, at the edge of block B5 a very porous layer with apparent closed pores is formed with a thickness of ~0.5 µm (Fig. **4**(h)). The porous layer is also present in between and beneath the fuzz ball at the edge of the blackish area on B4 (not shown), but not where the fuzz layer is completely formed (Fig. **4**(c,d)). The surface of this porous layer has some edgy topography, as shown in Fig. **4**(g)).

In addition, the fuzz layer seems to consist of two sub-layers with higher Mo content in the buried one (see e.g. Fig. **4**(e)). The ratio W to Mo resulting from the quantification of the EDX data for the top layer and lower layer in Fig. **4**(e)) is 8 and 3, respectively. The ratio shows a strong variation between the different cross-sections (Fig. **4**(a)) reaching even values below 1. This sub-layer structure probably reflects the transport of the W from the bulk to the surface, i.e. intermixing, as observed by [15] or some changes during the Magnum-PSI exposure.

3.5 Specials / Impurities

3.5.1 Prelude

Some remarkable observations were made in correlation to impurities deposited from the plasma beam. Molybdenum (Mo), copper (Cu), iron (Fe), chromium (Cr) and tin (Sn) are observed via optical emission spectroscopy in the plasma beam [6]. Note that the detected impurity amounts on the

surfaces are small compared to the acquired fluences (i.e. layers of about 100 nm contain about 10^{22} at/m^2; with sticking probability of 1 and without re-erosion, a fraction of $<<10^{-6}$ for impurities in the plasma beam can be estimated).

In any plasma devices, impurities are always present to some level, which are hardly to be quantified. For high fluence exposures, it has to be noted that already a very small fraction of, e.g., O and C (e.g. 10^{-6}) could lead to significant erosion even of W in a pure hydrogen plasma (depending on the electron temperature). Furthermore, high loads in the source could lead to an increase in impurity content in the plasma beam which could result, e.g., in W deposition [16] when a W electrode is used. Note Cu and Mo are used in the plasma source of Magnum-PSI. In addition, impurities can be generated by erosion of the sample holder (e.g. Fe/Cr), which is also exposed to an intense plasma. The plasma beam might redistribute sputtered material. All this lead to a complicated impurity deposition situation. Nevertheless, this will also happen in a fusion plasma device [16, 17, 18].

3.5.2 Tin

On top of the issues mentioned in section 3.5.1, in previous exposure campaigns of Magnum-PSI, a quite substantial amount of tin (Sn) was introduced into the chamber [19]. Unfortunately, this Sn seemed to be redistributed and deposited onto the mockup. Sn was detected in nearly all EDX analyses on the surface of the W monoblocks. Sn structures as observed in dedicated Sn plasma exposure experiment in another plasma device [20] are found on the mockup. These structures are Sn sponge-like structures with bubbles in the Sn branches (as observed for exposure just below the melting point of 505 K [20]) and Sn droplets with a contact angle of only about 45°. In particular they are observed on the sidewall in the gaps between the W monoblocks, e.g., Sn droplets on F4 & F5 (diameter of 10-50 µm) and Sn sponge on F6 (branch thickness of ~3 µm, branch length of >50 µm). In some cases, Sn is found incorporated in deposited structures and layers containing large fractions of Mo, Fe, and Cu.

3.5.3 Molybdenum

On all areas around the plasma beam centre (Figs. **3**(b,d,e)) **4**(e)), but also far away (Fig. **2**), Mo was observed. At some locations, the thickness of Mo-dominated layers was determined on FIB-prepared cross-sections, which is in the range of 50 nm (maximal observed of 100 nm). Note that a systematic analysis of the thickness across the samples was not performed.

Interestingly, the Mo distribution varies laterally (10s of µm) in areas showing large recrystallized grains on the surface. In elemental maps of the surface obtained by EDX, the grain structure is visible, i.e., the amount of Mo varies from grain to grain (Fig. **3**(b)). As these regions exhibit high temperatures, the mobility of Mo (and Sn) across the surface varies with grain orientation. In addition, the Mo diffusion along grain boundaries is enhanced compared to diffusion into grains as can be concluded from the observation of Mo-decorated grain boundaries observed on FIB-prepared cross-sections (Fig. **3**(d,e)). The Mo enrichment at the grain boundaries fades out at a depth of 2-3 µm. This behaviour could further be studied on the metallographic prepared cross-sections up to larger depth and along large length of cross-sections.

The nanostructured fuzz observed on block B4, contains also a large fraction of Mo (Fig. **4**(e)). Whether the Mo presence explains why fuzz formation is observed outside the typical existence window of W fuzz is unclear [10, 11]. Fuzz formation is also reported for Mo [21]. The temperature required for Mo fuzz formation is lower than for W [11, 21]. Furthermore, the growth of fuzz could also be promoted by the deposition of the Mo, similar to the observations in [22].

3.5.4 Copper and iron/chromium

Cu and Fe together with Cr are often significantly present. They sometimes even dominate the observed impurities. Trace of Cu and Fe were very frequently observed on all surfaces.

The dark areas at the edges of block B3 to block B2 are attributed to a layer dominated by Cu. Note that the exposure on B2 was the last one being performed. From the distribution of this Cu, it could be speculated that the Cu originated from the CuZrCr tube, e.g., by sputtering. This is supported by the observation that the Cu amount increase with depth from the surface on the side of block B3 in the gap. On the other hand, the temperature gradient may originates this variation, and the origin of the Cu is the plasma source.

The analyses of the blue-coloured area in Fig. **1** on F2 shown a Fe+Cr dominated layer. This large amount of Fe+Cr extents across the gap onto F3. In the centre of the exposure on F3, a double layer is observed, i.e., a >50 nm Mo-dominated layer is covered by a <50 nm Fe+Cr- dominated layer. This leads to the conclusion that the Fe+Cr producing event was after the exposure on F3, which was the first one of all.

4. Conclusion and Summary

A small-scale mockup of the ITER divertor plasma-facing units, consisting of seven tungsten monoblocks brazed on to a CuCrZr cooling tube, was exposed to a variety of high fluence, high flux plasma loads in Magnum-PSI [2, 3, 6]. Six exposures were performed including H, He, D and D:He (95:5) plasmas with low electron temperature (1.5-5 eV) and high electron density (1×10^{20}-2×10^{21} m^{-3}), resulting in a maximum surface temperature in the range 600-1200 °C (Tab. **1**) [6]. These exposures aimed to closely replicate the partially detached conditions expected at the divertor strike points during the different operational phases of the ITER staged approach [4]. The largest fluence, ~10^{30} D m^{-2}, achieved in 19 hours, is equivalent to around one year of full power operation, i.e., a few thousand discharges of 400 s duration [1].

The first step of the post-mortem analysis, with SEM, EDX and CLSM, is presented and aimed at studying how such long-term exposures affected the microstructure of each monoblock. The monoblocks behave as expected. No cracking (or melting) is observed. When the surface temperature exceeds ~1200 °C, as was the case in four exposures, recrystallization was observed. No strong erosion takes place, as the survival of the grinding grooves even in the recrystallized areas demonstrates. Furthermore, only the pure He exposure leads to surface topography changes of the surface layer at ~850 °C. The well-studied nanostructured fuzz is formed, despite the rather low ion energy (<18 eV) [10-15, 21, 22]. Probably, the observed Mo presence provokes the fuzz formation. The addition of He to D plasma at ~1200 °C does not lead to such surface changes; only recrystallization occurs.

The presence of impurities imply some complications for the analyses. Nevertheless, the impurity lead to some unexpected observations, e.g., the enhanced diffusion of Mo along the grain boundaries in the recrystallized areas and the sponge-like Sn structures [20]. Overall, the amount of impurities arriving with the plasma is small related to the high accumulated fluences, and the impurities do not harm the positive performance for the different high fluence exposure conditions, i.e., these experiments do not emphasize any additional concerns for the different exposure conditions in the ITER staged approach.

The observations for these high fluence exposures on a small-scale ITER plasma facing unit mockup indicate that no catastrophic behaviour appeared and that such components are capable of fulfilling their design goals.

Acknowledgment

The actively-cooled monoblock chain was supplied by the ITER Organization and F4E as part of a EUROfusion-funded experiment to investigate the effect of ITER-relevant fluences on the properties of tungsten. This work has been carried out within the framework of the EUROfusion Consortium and has received funding from the Euratom research and training programme 2014-2018 and 2019-2020 under grant agreement No 633053. Work partly performed under EUROfusion WP PFC. The views and opinions expressed herein do not necessarily reflect those of the European Commission or of the ITER Organization.

References

[1] De Temmerman G, Hirai T, Pitts RA 2018 *Plasma Phys. Control. Fusio*n **60** 044018.

[2] van Eck HJN et al. 2019 *Fusion Eng. Des.* in press

[3] van de Pol et al. 2018 *Fusion Eng. Des.* **136** 597-601

[4] ITER Organisation 2018 Research Plan within the Staged Approach *ITER Technical Report* **ITR-18-003** https://www.iter.org/technical-reports

[5] Brezinsek S et al. 2017 *Nuclear Fusion* **57** 116041

[6] Morgan TW, Schwarz-Selinger T, Balden M, Li Y, Rosas Saad JA, Loewenhoff T, Wirtz M, Sietsma J, Brezinsek S, De Temmerman G 2019 ITER monoblock performance under lifetime loading conditions in Magnum-PSI, *Presented at 17th PFMC, Eindhoven, May 2019, submission to Nuclear Fusion in preparation*

[7] Hirai T et al. 2015 *J. Nucl. Mater.* **463** 1248-51

[8] Loewenhoff T et al. 2015 *Nuclear Fus.* **55** 123004

[9] van den Berg MA et al. 2013 *J. Nucl. Mater.* **438** S432-4

[10] Kajita S, Sakaguchi W, Ohno N, Yoshida N, Saeki T 2009 *Nucl. Fusion* **49** 095005

[11] Kajita S et al. 2018 *Surf. Coat. Technol.* **430** 86-92

[12] Greuner H et al. 2014 *J. Nucl. Mater.* **455** 681-4

[13] Hwangbo D, Kajita S, Tanaka H, Ohno N 2019 *Nucl. Mater. Energy* **18** 250-7

[14] Woller KB, Whyte DG, Wright GM 2017 *Nucl. Mater. Energy* **12** 1282-7

[15] Doerner RP, Nishijima D, Krasheninnikov SI, Schwarz-Selinger T, Zach M 2018 *Nucl. Fusion* **58** 066005

[16] Balden M, Lindig S, Manhard M, Krieger K, ASDEX Upgrade Team 2013 *J. Nucl. Mater.* **438** S220-3

[17] Mayer M, Likonen J, Coad JP, Maier H, Balden M, Lindig S, Vainonen-Ahlgren E, Philipps V, JET-EFDA Contributors 2007 *J. Nucl. Mater.* **363-365** 101-106

[18] Kallenbach A et al, 2011 *J. Nucl. Mater.* **415** S19-26

[19] Morgan TW et al. 2018 *Plasma Phys. Control. Fusion* **60** 014025

[20] Manhard M, Schwarz-Selinger T, Balden M, Dürbeck T, Maier H, Neu R 2019 Erosion and Deuterium Uptake of Solid and Liquid Tin in a Low-Temperature Deuterium Plasma, *Presented at 17th PFMC, Eindhoven, May 2019, submission to Nuclear Fusion in preparation*

[21] Takamura S 2014 *Plasma Fus. Res.* **9** 1405131

[22] Kajita S, Kawaguchi S, Yoshida N, Ohno N, Tanaka H 2018 *Nucl. Fusion* **58** 106002

Table

Tab. 1: Exposure conditions in Magnum-PSI onto the small-scale ITER W monoblock mockup. The max values are valid for the beam centre. The electron temperature and density are in the range 1.5-5 eV and 1-20×10^{20} m^{-3}.

Block	Order of exposures	Centre of exposure on	Exposure on front/back	Plasma species	Max $T_{surf,}$ (°C)	Max Fluence (m^{-2})	Max Flux ($m^{-2}s^{-1}$)	Duration (h)	Number of interruption
1			None						
2	6	B2	Back	D	1235	3.2×10^{29}	7.8×10^{24}	11.2	1
3	1	F3	Front	H	635	7.7×10^{28}	9.3×10^{23}	22.6	2
4	5	B4	Back	He	860	1.9×10^{28}	2.2×10^{24}	2.9	0
5	2	F5	Front	D	1245	7.7×10^{29}	1.0×10^{25}	19.7	2
6	4	B6	Back	D:He (95:5)	1225	3.9×10^{29}	1.0×10^{25}	17.8	2
7	3	F7	Front	D:He (95:5)	1240	2.2×10^{29}	9.3×10^{24}	6.5	0

Figures

Fig. 1: Photos of the two plasma-exposed faces, **(a)** "Front" and **(b)** "Back", of the small-scale ITER W monoblock mockup. The centre of the plasma beams, i.e., the position of max T_{surf} in Tab. **1**, and the analyses positions are marked (imaging of surface: SEM; imaging of FIB-prepared cross-sections: CS; elemental mapping: EDX; detailed digital microscopy with roughness measurement: CLSM).

Fig. 2: **(a)** top view SEM image of an "unexposed" area, i.e., the centre of F1, showing the grinding grooves of the technical surface of the monoblocks and **(b)** a FIB-prepared cross-section illustrating the zone with small and distorted W grains below the surface (position of cross-section marked in (a)). The elemental composition of the thin black line visible in the cross-section (b) was determined by EDX as dominated by Mo. Note the cross-section is viewed under an angle of 36°.

Fig. 3: **(a)** top view SEM image of the beam centre of exposure F5, ~10^{30} D/m^2 at T_{surf} of 1245 °C visualizing large recrystallized grains. **(b)** the elemental intensity maps (EDX) of W, Mo and Sn of the region of (a) illustrating the grain dependent decoration of W grains by the deposited impurities. **(c)** FIB-prepared cross-section, which is shown as a scaled overlay in (a), too. **(d)** and **(e)** magnified parts of the region left and in the middle of (c), respectively. As inserts, the elemental intensity maps of a part of the areas shown in (d) and (e) clearly indicate the decoration of the grain boundaries with Mo and a Mo-dominated layer of 50 nm on the surface. Note the cross-section is viewed under an angle of 36°.

Fig. 4: **(a)** photo of the spot of exposure B4, 2.2×10^{28} He/m^2 at 860 °C with labelling of analysed positions; **(b)** top view SEM image of beam centre showing the filigrane tendrils of the fuzz; **(c)** SEM image of the cross-section at the edge of the beam; **(d)** SEM image of the cross-section very close to the edge of block B4 (see (a)), but also close to the beam centre; **(e)** elemental intensity map of the region of (d); **(f)** top view SEM image of the edge of the spot with "fuzz-balls" of ~10 µm height and ~20-30 µm diameter; **(g)** top view SEM image of the region between the "fuzz balls" (position marked in (f); **(h)** SEM image of the cross-section very close to the edge of block B5 (distance to cross-section shown in (d,e) is only 0.8 mm). Note the cross-sections are viewed under an angle of 36°.

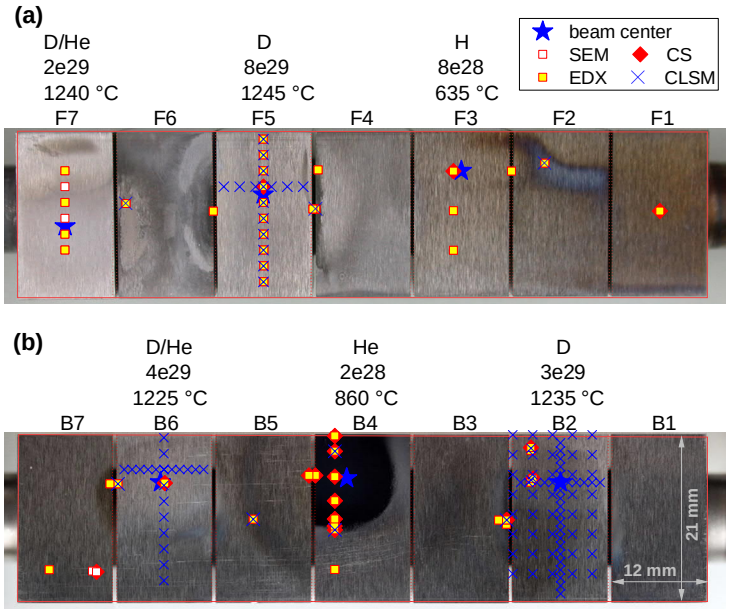
(a)
D/He
2e29
1240 °C
D
8e29
1245 °C
H
8e28
635 °C
beam center
SEM
CS
EDX
CLSM
F7
F6
F5
F4
F3
F2
F1
(b)
D/He
4e29
1225 °C
He
2e28
860 °C
D
3e29
1235 °C
B7
B6
B5
B4
B3
B2
B1
21 mm
12 mm

Fig. 1

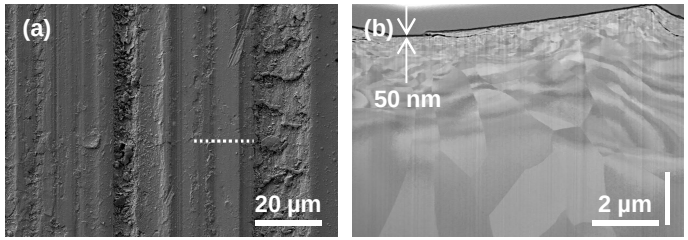
(a)
20 µm
(b)
50 nm
2 µm

Fig. 2

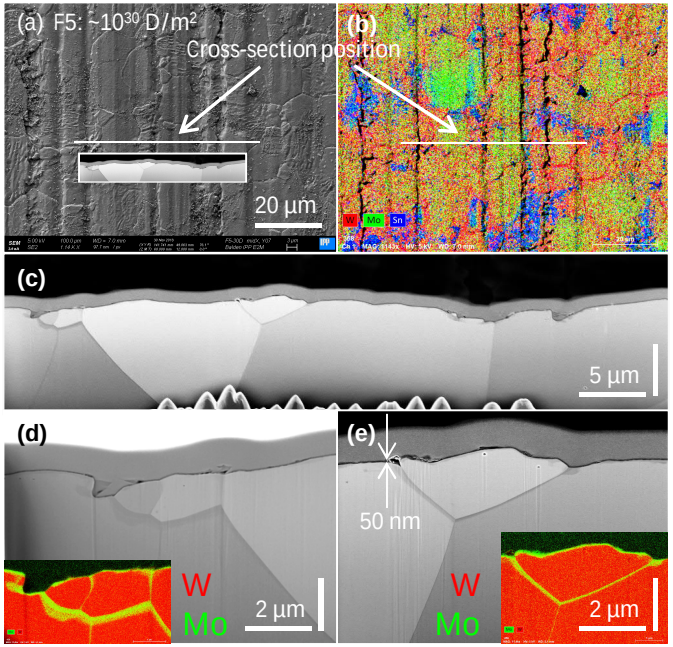
(a) F5: ~10^30 D/m²
Cross-section position
20 µm
(b)
W
Mo
Sn
(c)
5 µm
(d)
W
Mo
2 µm
(e)
50 nm
W
Mo
2 µm

Fig. 3

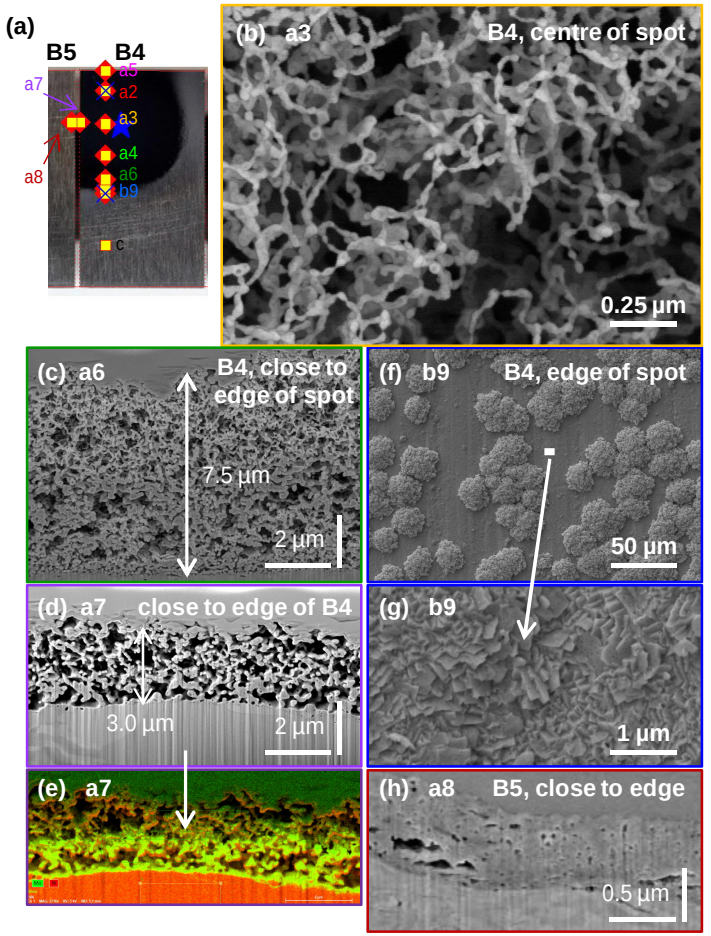
(a)
B5
B4
a7
a8
a5
a2
a3
a4
a6
b9
c
(b) a3
B4, centre of spot
0.25 µm
(c) a6
B4, close to edge of spot
7.5 µm
2 µm
(f) b9
B4, edge of spot
50 µm
(d) a7
close to edge of B4
3.0 µm
2 µm
(g) b9
1 µm
(e) a7
(h) a8
B5, close to edge
0.5 µm

Fig. 4